# Transverse Viscoelastic Properties Of Cellulosic Fibers Investigated By Atomic Force Microscopy

**Caterina Czibula** (Institute of Physics, Montanuniversitaet Leoben; CD Laboratory for Fiber Swelling and Paper Performance, Graz University of Technology), **Christian Ganser** (Institute of Physics, Montanuniversitaet Leoben; CD Laboratory for Fiber Swelling and Paper Performance, Graz University of Technology), **Christian Teichert** (Institute of Physics, Montanuniversitaet Leoben; CD Laboratory for Fiber Swelling and Paper Performance, Graz University of Technology), **Ulrich Hirn** (Institute of Paper, Pulp and Fibre Technology, Graz University of Technology; CD Laboratory for Fiber Swelling and Paper Performance, Graz University of Technology)

## ABSTRACT

Pulp fibers have not only anisotropic properties, but also exhibit a very rough surface due to their hierarchical structure. For this reason, an atomic force microscopy (AFM) method was developed to overcome the limitations due to the surface roughness of the pulp fibers and to provide comparable results of local viscoelastic properties in transverse direction at different relative humidity (RH) and in water. The evaluation of the experimental data combines contact mechanics and viscoelastic models which consist of springs and dashpots in series or parallel describing elastic and viscous behavior, respectively. Here, it will be demonstrated that the so-called Generalized Maxwell model of order two (GM2) yields reasonable results for two kinds of single fibers, viscose and pulp fibers, at different RH values and in water. Both fiber types show the same trend. The moisture changes at different RH lead to a steady decrease of the elastic and viscous parameters of the GM2 model with increasing RH. In water, however, all parameters show a jump-like drop by about two orders of magnitude indicating that the viscoelastic behavior in water is different.

## INTRODUCTION

Dynamic loading is very common during printing, converting, and some end-use scenarios of paper. Mechanical simulation of paper converting and end-use processes are becoming an increasingly relevant tool in the paper converting industry. Therefore, it is of considerable interest to gain more experimental insight on how mechanical properties of cellulose fibers are related to properties of end-products like paper. Our work focusses on the transverse viscoelastic behavior of single cellulosic fibers investigated at varying RH.

In general, investigations of the mechanical properties in transverse fiber direction, are scarce. One reason is that it is still difficult to access the transverse mechanical properties of fibers experimentally. Earlier investigations of the transversal elastic modulus were based on lateral compression of wet fibers [1-3].

Recently, AFM [4] methods have enabled the investigation of local properties and made it possible to access the fiber surface on the nanoscale. Apart from offering the possibility to characterize the surface morphology of fibers in detail [5-7], the AFM probe is a force sensor with high sensitivity. The single-fiber properties of wet fibers have been investigated with AFM methods numerous times. Here, the flexibility [8] and conformability [9], as well as the creep behavior of wet fiber surfaces of hardwood chemi-thermo-mechanical pulp, and softwood kraft pulp [10] have been studied. A comprehensive study of the mechanical properties of pulp and viscose fibers at different RH has been obtained with AFM based nanoindentation (AFM-NI) under controlled humidity [11, 12].

For pulp fibers, no information on the transversal viscoelastic properties has been reported so far. Also, viscose fibers have not been investigated in transverse direction, although they exhibit more homogeneous properties and a smoother surface. For wood, on the other hand, the viscoelastic behavior of pine specimens along the grain [13] and of green wood in transverse direction [14] has been investigated.

In this work, the creep compliance of single pulp and viscose fibers in transverse direction has been investigated on the nanoscale employing contact mechanics in combination with a rather simple linear viscoelastic model. A comprehensive validation of this method has been carried out with the well-known polymers polycarbonate and poly(methylmethacrylate) [15]. The obtained AFM measurement results were compared to tensile testing and nanoindentation to prove the reliability of the method. Here, comparable results of local viscoelastic properties at different RH values for pulp and viscose fibers are presented for a GM2 model. The results are presented by the parameters $E_\infty$, $E_1$, and $E_2$ describing elastic behavior and the viscosities $\eta_1$ and $\eta_2$ which are characterizing viscous behavior. Additionally, two relaxation times, $\tau_1$ and $\tau_2$, and the instantaneous modulus $E_0$ can be helpful to interpret the relaxation behavior.

## EXPERIMENTAL

### Atomic force microscopy

The measurements in this work have been acquired with an Asylum Research MFP-3D AFM. The instrument is equipped with a closed-loop planar x-y-scanner with a scanning range of 85 µm x 85 µm and has a z-range of about

15 µm. For the viscoelastic measurements, LRCH silicon probes (Team Nanotec, Germany) with a hemispherical tip (radius of about 300 nm) have been used. The large tip radius enabled the investigation of a larger surface area. Another advantage of such an AFM probe is that higher forces can be applied, and the indentation depths and strains still remain low. To measure at controlled humidity, an AFM fluid cell was employed. With nitrogen flow through a home-built setup, the desired humidity levels can be reached. However, due to condensation effects, the maximum RH reached for these experiments were 80 % RH. Above 80 % RH it is very difficult to guarentee stable humidity conditions.

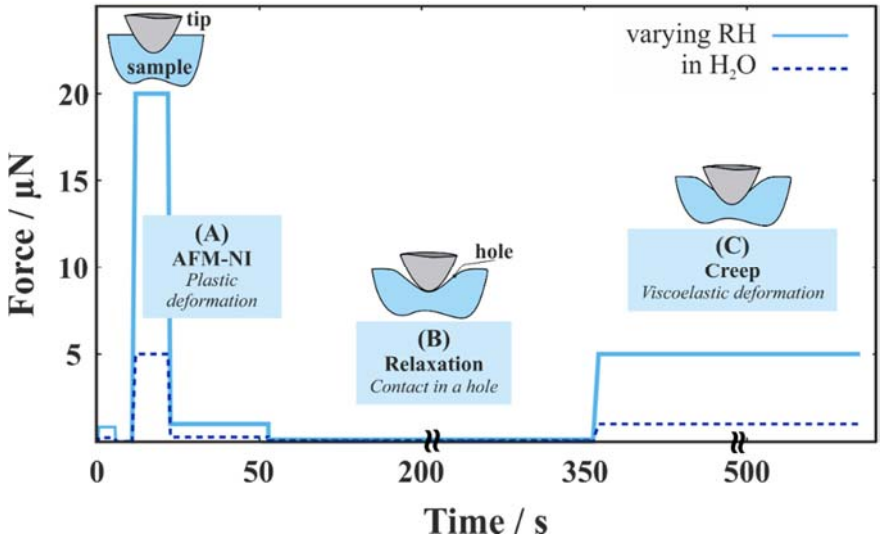


*Fig. 1. Applied load schedule for the measurements at varying RH (solid line) and for the measurements in water (dashed line). The load schedule consists of three parts. In part (A), the fiber surface is plastically deformed and afterwards, in (B), relaxes for 300 s. In part (C), a creep curve is recorded, and the viscoelastic response is tested for 240 s. The icons in (A), (B), and (C) indicate the tip – sample interaction at the different loads.*

The load schedule for determining the viscoelastic properties is presented in Fig. 1. It consists of three main parts (A, B, C) which are explained in more detail in [15, 16]. In Fig.1 (A), a high load of 20 µN (5 µN in $H_2O$) is applied for 10 s followed by a small unloading force for 30 s to introduce plastic deformation to the sample surface. This way, a defined contact area between tip and surface is created and local roughness is reduced due to this deformation. Here, also values for the reduced modulus $E_r$ and the hardness $H$ according to the method of Oliver and Pharr [17] are obtained. Now, the contact between tip and surface can be described as contact in a hole, as indicated in Fig. 1 (B). Afterwards the surface relaxes for 300 s and the tip stays in contact to the surface with a small force of about 300 nN. In the final and most important part for the viscoelastic evaluation (Fig. 1 (C)), a load of 5 µN (1 µN in $H_2O$) with a loading rate of 3.2 µN $s^{-1}$ is applied for 240 s, and the viscoelastic response or creep is measured. The obtained creep curves are used for the evaluation of the viscoelastic properties.

**Contact mechanics and adhesion**

A contact mechanics model is required to relate the force and indentation depth measured in the AFM experiment to stress and strain needed for the viscoelastic model. Since it was found that adhesion during the experiments varies between 100 and 900 nN, it cannot be neglected. The Johnson-Kendall-Roberts (JKR) model [18] applies especially to the contact of a large radius probe with a soft sample surface [19], and it considers adhesion. It was assumed that the underlying material is isotropic. Details on how the JKR and the viscoelastic model are combined and a study on the influence of adhesion are described in [15].

**Viscoelastic model**

In this work, viscoelasticity is represented with linear differential equations. Different parallel or serial combinations of Hookean elastic springs (denoted elastic moduli $E_i$) and Newtonian viscous dashpots (denoted viscosities $\eta_i$) describe elastic and viscous behavior, respectively [20]. Here, the Generalized Maxwell model of order two (GM2) proved to be appropriate and is presented in Fig. 2. It consists of three springs ($E_\infty$, $E_1$, $E_2$) and two dashpots ($\eta_1$, $\eta_2$). $E_\infty$ corresponds to a purely elastic response at infinitely slow loading, whereas the instantaneous elastic modulus $E_0$ corresponds to an infinitely fast loading. Both dashpots become rigid, and only the springs deform: $E_0 = E_\infty + E_1 + E_2$.

The combination of spring and dashpot in series ($E_1$ and $\eta_1$, $E_2$ and $\eta_2$) are so-called Maxwell elements, and for each of these elements a relaxation time $\tau_i$ can be defined. It is the ratio between viscosity $\eta_i$ and elastic modulus $E_i$ of the $i^{th}$ Maxwell element. More details are presented in [15, 16].

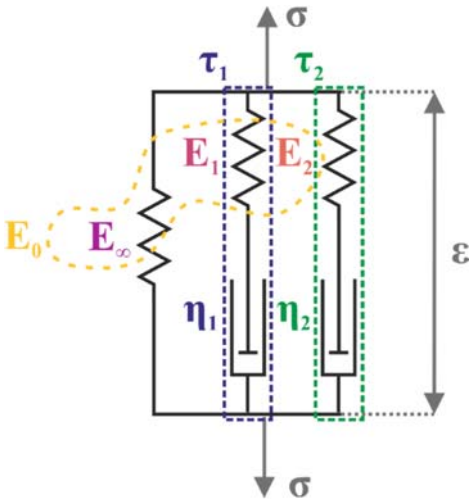


*Fig. 2. Generalized Maxwell model of order 2 (GM2). It consists of three springs $E_\infty$, $E_1$, $E_2$ and two dashpots $\eta_1$, $\eta_2$. An instantaneous elastic modulus $E_0$ can be defined at infinitely fast loading: $E_0 = E_\infty + E_1 + E_2$. Each dashpot is in series with and forms a so-called Maxwell element. For each of these elements a relaxation time $\tau_i$ can be defined, which is the ratio between viscosity $\eta_i$ and elastic modulus $E_i$ of the $i^{th}$ Maxwell element.*

**Sample preparation**

The investigated single fiber samples were flat viscose fibers (Kelheim Fibres, Germany) with a rectangular cross-section of 200 µm width and 5 µm thickness, and industrial, unbleached (κ = 42), once dried and unrefined softwood kraft pulp fibers (Mondi Frantschach, Austria). These pulp fibers are a mixture of spruce and pine with a length between 3 – 5 mm and a diameter of about 20 – 30 µm. For the investigation of the mechanical properties with AFM, it is crucial that the fibers are fixed to a substrate and prevented from bending during load application. This is achieved by gluing the fiber with nail polish on a steel sample holder [21, 22]. To ensure that the fibers are tested in equilibrium moisture content, the samples were equilibrated overnight for at least eight hours at the desired relative humidity level. For measurements in water, the fibers were immersed in water about 24 hours before testing.

**RESULTS**

**Fitting of the experimental data**

Representative 5 x 5 µm² AFM topography images of a pulp and a viscose fiber surface at 60 % RH are presented in Fig. 3. On these surface areas, individual measurement points were selected for the viscoelastic experiment. The topography of the pulp and viscose fibers is presented before (Fig. 3a,c) and after (Fig. 3c,d) the AFM experiment. It should be noted that these images have been recorded with a large radius probe, therefore, single fibrils and features with smaller sizes are not clearly resolved. The pulp fiber has a very rough surface which is characterized by wrinkle-like structures. These wrinkles are in the same lateral size range as the AFM tip diameter which is indicated by blue dots. Compared to that, the viscose fiber surface appears smooth with well-aligned wrinkles and characteristic trenches. For the pulp fibers, mostly the surface of the S1 layer is investigated which was confirmed in morphological studies with AFM [23]. This is due to the fact that during kraft pulp processing most of the primary wall layer is removed due to its high lignin content. The viscoelastic experiment has been performed on rather smooth positions of the surfaces. Single positions on the pulp and viscose fiber are indicated in Fig. 3a and c with the blue dots. It should be mentioned for the pulp fiber surface that during measurement lateral movement of the wrinkles cannot be excluded. However, it is assumed that most of this movement is taking place during the plastic deformation. There, a four times higher load is applied than during viscoelastic testing.

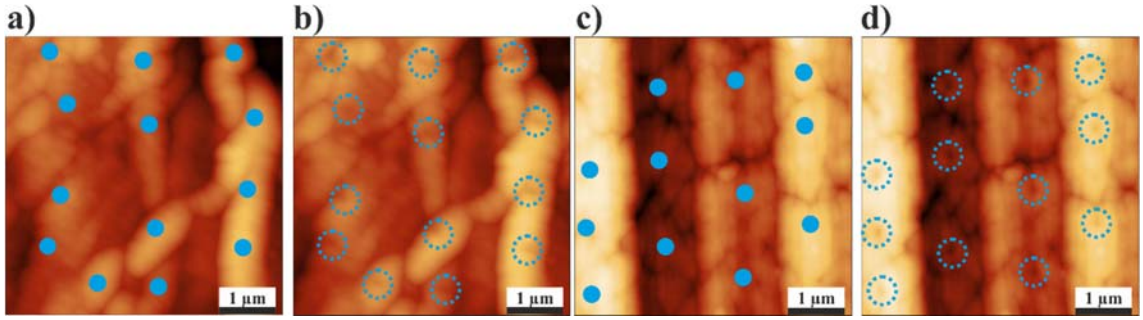


*Fig. 3. 5 µm x 5 µm AFM topography images for pulp (a, b) and viscose (c, d) fibers at 60 % RH. Topography image of the same position on a pulp fiber surface (a) before and (b) after the viscoelastic testing experiment (z-scale: 900 nm). (c) Topography image of the same position on a viscose fiber surface (c) before and (d) after the experiment (z-scale: 350 nm). The blue dots indicate measurements points with the dot size corresponding to the diameter of the hemispherical AFM tip. The blue dashed circles mark the permanent holes after the experiment.*

Experimental creep curves with corresponding GM2 fits at different RH are presented for pulp and viscose fibers in Fig. 4. For pulp fibers, in Fig. 4a, curves at 10 %, 25 %, 45 %, 60 %, and 75 % RH have been recorded. The indentation depth increases with increasing RH, ranging from about 10 – 100 nm. The same trend is apparent for the viscose fibers (Fig. 4b), but the indentation depth is much lower. For 35 %, 60 %, and 80 % RH, the AFM is only penetrating 10 – 50 nm into the surface of the viscose fibers. Since experiments with indentation depths smaller than 10 nm show an influence of signal noise, no measurements for viscose fibers at lower RH than 35 % have been performed [15, 16]. In general, the GM2 model fits the data at different RH very well, with slight deviations at high RH. For measurements of the pulp fibers in water, the situation is different. The GM2 fits show deviations, and a third relaxation time is needed to describe the behavior in a more satisfying way. This will be discussed in more detail for pulp fibers in [16]. A similar behavior in water was not found for viscose fibers. Although the indentation depth increases to 300 nm at the much lower load of 1 µN, the GM2 model still fits the data well [15].

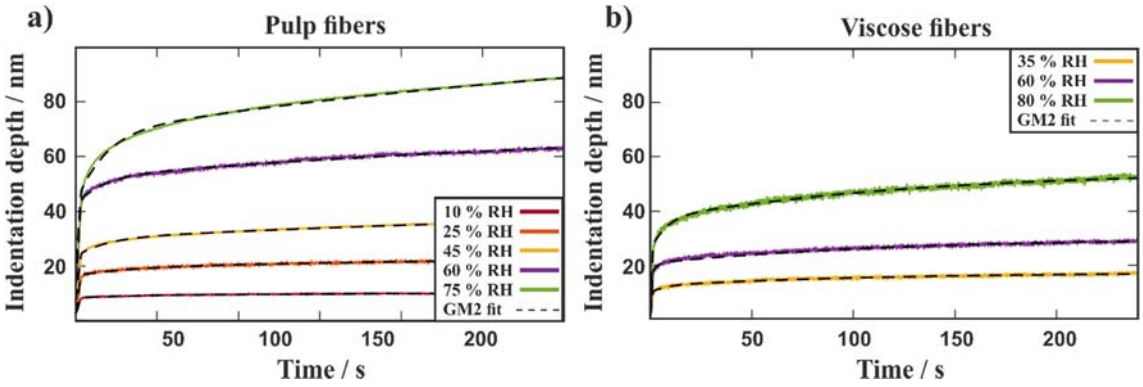


*Fig. 4. (a) Representative experimental creep curves at 10 %, 25 %, 45 %, 60 %, and 75 % RH for pulp fibers with the corresponding fit curves as black dashed lines. (b) Representative experimental creep curves at 35 %, 60 %, and 80 % RH for viscose fibers with the corresponding fit curves as black dashed lines.*

**Comparison of the viscoelastic properties of pulp and viscose fibers at different RH and in $H_2O$**

In Fig. 5 the results for the viscoelastic properties at different RH and in water from the GM2 model are presented for pulp and viscose fibers. For each RH and water value at least 30 single measurement points for every fiber type have been evaluated. Fig. 5a, presents a comparison of the elastic moduli $E_\infty$, $E_0$. Here, pulp and viscose fibers show a slightly decreasing trend from 10 % to 75 % RH and from 35 % to 80 % RH, respectively. Immersed in water, both fibers exhibit the same drop of factor 100 compared to the lowest measured RH. Viscose fibers have at intermediate RH slightly higher elastic moduli than pulp fibers, but in water they exhibit a decrease to lower values than pulp fibers. In Fig. 5b and 5c, the viscous behavior is characterized by the viscosities $\eta_1$, $\eta_2$. Here, both fibers again show a slight decrease with increasing RH and a more pronounced decrease immersed in water. Especially the results for the viscose fibers show little change between 35 % and 80 % RH, compared to the pulp fibers which decrease by one order of magnitude. In water, $\eta_1$ and $\eta_2$ of the viscose fibers are lower than for the pulp fibers.

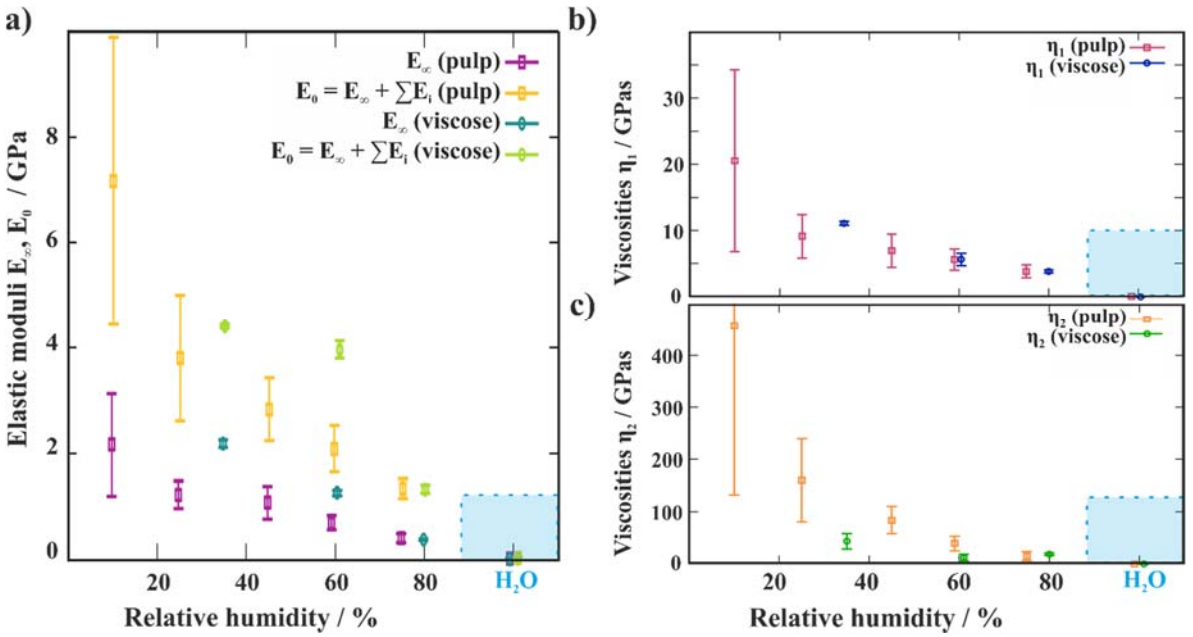


*Fig. 5. Results obtained by the GM2 model for pulp and viscose fibers. In (a) the elastic parameters $E_\infty$, $E_0$ are presented and in (b) the viscous parameters $\eta_1$, and (c) $\eta_2$ are depicted. The squares and spheres indicate the results for pulp and viscose fibers, respectively.*

For fibers immersed in water, the drop in elastic moduli and viscosities parameters of the GM2 model indicates that the behavior of both fiber types is different in water compared to changing RH. This pronounced decrease was already found with AFM-NI investigations [11, 12]. We observe for pulp fibers that the GM2 model is not sufficient to describe the relaxation behavior properly, an extension of the GM model will be presented and discussed in detail elsewhere [16].

In Table 1, an overview of literature values for the transverse elastic modulus of different fiber types measured in water is presented. Different experimental measurement techniques have been applied, like compression testing, osmotic swelling, or several AFM-based approaches. Comparison of the values for $E_0$ obtained with the GM2 model for the pulp (28 MPa) and the viscose (22 MPa) reveals that most of the results obtained from AFM-based methods [8, 9, 12] are in good agreement with each other. This, in a way, verifies also our viscoelastic method.

*Table 1: Overview of literature values for the transverse elastic modulus of varying fiber types measured in water obtained with different experimental techniques.*

| Fiber type | Transverse elastic modulus / MPa | Experimental technique | Literature |
|---|---|---|---|
| **spruce kraft pulp, κ = 42, earlywood, unbeaten** | 560 | macroscopic transverse compression | [2] |
| **spruce kraft pulp, κ = 42, earlywood, beaten** | 440 | | [2] |
| **Black spruce kraft and TMP, loblolly pine TMP** | 6.5-9.3 | macroscopic transverse compression | [3] |
| **Bleached softwood kraft pulp, κ = 1.2** | 1-12 | fiber flexibility (AFM) | [8] |
| **Unbleached, refined TMP pulp** | 15-190 | | [8] |
| **Spruce kraft pulp, κ = 61, unbeaten** | 13 | fiber conformability (AFM) | [9] |
| **TCF bleached softwood kraft, unbeaten** | 7 | | [9] |
| **Spruce thermo-mechanical pulp** | 182 | fiber conformability (AFM) | [10] |
| **Spruce and pine kraft pulp, κ = 42, unrefined** | 32 | AFM based nanoindentation | [12] |
| **Viscose** | 50 | | [12] |
| **Low-yield spruce kraft, rewetted, unbeaten** | 4 | osmotic swelling | [24] |
| **Spruce and pine kraft pulp, κ = 42, unrefined** | 28 | viscoelasticity (AFM) | [This work] |
| **Viscose** | 22 | | [This work] |

## CONCLUSIONS

The viscoelastic propertis of pulp and viscose fibers in transverse direction have been investigated with an atomic force microscopy-based method. In this work, the combination of contact mechanics with a viscoelastic GM2 model enabled the measurement of local creep curves on both fiber types at different RH, ranging from 10 % RH to 80 % RH and in water. Moreover, the GM2 model provides for pulp as well as viscose fibers good comparability of the transversal viscoelastic behavior between the different RH. In general, both fiber types show the same trend for the elastic and viscous values. All the results for the parameters of the elastic and viscous behavior show a gradual decrease until the highest RH level. For fibers immersed in water, the decrease is even more pronounced, indicating that the mechanical behavior and, therefore, the interaction of the fibers with water is different. This finding will be further discussed for pulp fibers in [16]. So far, the results of the elastic moduli values for the wet pulp and viscose fiber are in good agreement with literature values which were also obtained with AFM-based experiments.

## ACKNOWLEDGMENTS

The members of the CD-Laboratory for Fiber Swelling and Paper Performance gratefully acknowledge the financial support of the Austrian Federal Ministry of Economy, Family and Youth and the National Foundation for Research, Technology and Development. We also thank our industrial partners Mondi, Océ, Kelheim Fibres, and SIG Combibloc for their financial support.

## REFERENCES

1. Dunford, J., and Wild, P., "Cyclic transverse compression of single wood-pulp fibres," J. Pulp Pap. Sci., 28(4):136-141 (2002).
2. Hartler, N., and Nyrén, J., "Transverse Compressibility of pulp fibers. 2. Influence of cooking method, yield, beating, and drying," Tappi, 53(5):820-823 (1970).
3. Wild, P., Omholt, I., Steinke, D., and Schuetze, A., " Experimental characterization of the behaviour of wet single wood-pulp fibres under transverse compression," J. Pulp Pap. Sci., 31(3):116-120 (2005).
4. Binnig, G., Quate, C. F., and Gerber, C., "Atomic force microscope," Phys. Rev. Lett., 56(9):930 (1986).
5. Chhabra, N., Spelt, J., Yip, C., and Kortschot, M., "An investigation of pulp fibre surfaces by atomic force microscopy," J. Pulp Pap. Sci., 31(1):52-56 (2005).
6. Fahlén, J., and Salmén, L., "Pore and Matrix Distribution in the Fiber Wall Revealed by Atomic Force Microscopy and Image Analysis," Biomacromolecules, 6(1):433-438 (2004).
7. Schmied, F. J., Teichert, C., Kappel, L., Hirn, U., and Schennach, R., " Analysis of precipitated lignin on kraft pulp fibers using atomic force microscopy," Cellulose, 19(3):1013-1021 (2012).
8. Pettersson, T., Hellwig, J., Gustafsson, P.-J., and Stenström, S., "Measurement of the flexibility of wet cellulose fibres using atomic force microscopy," Cellulose, 24(10):4139-4149 (2017).
9. Nilsson, B., Wagberg, L., and Gray, D., "Conformability of wet pulp fibres at small length scales," In: *Proc. 12th Fundamental Research Symposium* (Oxford), 211–224 (2012).
10. Yan, D., and Li, K., "Conformability of wood fiber surface determined by AFM indentation," J. Mater. Sci., 48(1):322-331 (2013).
11. Ganser, C., Hirn, U., Rohm, S., Schennach, R., and Teichert, C.," AFM nanoindentation of pulp fibers and thin cellulose films at varying relative humidity," Holzforschung, 68(1):53-60 (2014).
12. Ganser, C., and Teichert, C., "AFM-based Nanoindentation of Cellulosic Fibers," in *Applied Nanoindentation in Advanced Materials*, ed. A. Tiwari (Wiley), 247–267 (2017).
13. Penneru, A. P., Jayaraman, K., and Bhattacharyya, D., "Viscoelastic behaviour of solid wood under compressive loading," Holzforschung, 60(3):294-298 (2006).
14. Bardet, S., and Gril, J., "Modelling the transverse viscoelasticity of green wood using a combination of two parabolic elements," Comptes Rendus – Mec., 330(8):549-556 (2002).
15. Ganser, C., Czibula, C., Tscharnuter, D., Schöberl, T., Teichert, C., and Hirn, U., " Combining adhesive contact mechanics with a viscoelastic material model to probe local material properties by AFM," Soft Matter, 14(1):140-150 (2018).
16. Czibula, C., Ganser, C., Seidlhofer, T., Teichert, C., Hirn, U., "Transverse viscoelastic properties of pulp fibers investigated by atomic force microscopy," submitted to J. Mater. Sci.
17. Oliver, W. C., and Pharr, G. M., "An improved technique for determining hardness and elastic modulus using load and displacement sensing indentation experiments," J. Mater. Res., 7(6):1564-1583 (1992).
18. Johnson, K. L., Kendall, K., and Roberts, A. D., "Surface Energy and the Contact of Elastic Solids," Proc. R. Soc. A Math. Phys. Eng. Sci., 324(1558):301-313 (1971).
19. Klapetek, P., "*Quantitative Data Processing in Scanning Probe Microscopy,"* Amsterdam: Elsevier (2013).

20. Flügge, W., "*Viscoelasticity,"* Berlin: Springer (1975).
21. Fischer, W. J., Zankel, A., Ganser, C., Schmied, F. J., Schroettner, H., Hirn, U., " Imaging of the formerly bonded area of individual fibre to fibre joints with SEM and AFM," Cellulose, 21(1):251-260 (2014).
22. Schmied, F. J., Teichert, C., Kappel, L., Hirn, U., Bauer, W., and Schennach, R., "What holds paper together: Nanometre scale exploration of bonding between paper fibres," Sci. Rep., 3(1):2432 (2013).
23. C. Ganser, "Surface characterization of cellulose fibers by atomic force microscopy in liquid media and under ambient conditions," Diploma Thesis, Montanuniversitaet Leoben (2011).
24. Scallan, A., Tigerström, A., "Swelling and elasticity of the cell wall of pulp fibres," J. Pulp Pap. Sci., 18(5):188-193 (1992).